

Production and Characterization of GRC-SWCNT Composites for Shell Elements

Serkan SUBASI¹ *, Heydar DEHGHANPOUR², Muhammed MARASLI²

¹ Düzce University, Engineering Faculty, Civil Engineering Department, Düzce, Turkey 81620

² Fibrobeton Company, Building Materials Research and Development, Istanbul, Turkey 34810

crossref <http://dx.doi.org/10.5755/j02.ms.29008>

Received 27 April 2021; accepted 25 January 2022

Nano-sized defects in Glass fiber Reinforced Concrete (GRC) shell elements can cause damage over time, leading to mechanical and durability problems. Therefore, in this study an experimental program was conducted to investigate the application of single-walled carbon nanotube as a nano-additive material in GRC. Since there is no study on GRC-carbon nanotube (CNT) composites in the literature, the behavior of CNTs on conventional concretes was discussed. Five different GRC-SWCNT composite mixtures containing 0, 0.007, 0.010, 0.015 and 0.020 wt.% single walled carbon nanotube (SWCNT) were obtained. Calcined kaolin and acrylic polymer were used as pozzolanic and chemical modification materials in the mixtures, respectively. Workability, density, capillarity, pressure, flexural, tensile, impact, Leeb hardness and FE-SEM tests of the produced samples were carried out. According to the results obtained, the optimum SWCNT ratio in GRC mixtures was found to be 0.015 %. It was observed that there was a linear relationship between the mechanical results. FE-SEM images confirmed that SWCNTs act as bridges for micro-cracks and reinforce the microstructure.

Keywords: glass fiber, GRC, carbon nanotube, SWCNT, shell elements, mechanical properties.

1. INTRODUCTION

Alkali resistant glass fiber (AR-GF) has been used for different purposes in building materials in recent years and attracts the attention of many researchers [1, 2]. AR-GFs contain 15–20 % ZrO₂ and this significantly protects the fibers against alkalis in the hydrated cement paste [3, 4]. In previous studies, AR-GFs have proven positive effects on building materials in many aspects such as splitting tensile strength [5, 6], modulus of rupture [7], flexural strength [8], and abrasion resistance [9].

The main uses for GRCs are generally cladding panels, due to their satisfactory mechanical properties and fire resistance [4, 10]. Among other non-structural applications of GRCs, areas such as permanent formwork, sewer lining, building restoration, tunnel lining and acoustic barrier can be pointed out [11]. GRCs also have a limited number of uses in structural applications [12]. Besides many superior properties of GRCs, there are also problems such as embrittlement [13]. Micro-sized AR-GFs prevent the formation of micro-cracks, but nano-sized cracks may develop over time and threaten the mechanical and durability properties of GRC elements. Different solutions have been proposed by many researchers to address these problems of GRCs. Protective layer coatings for aged GRCs [14] and adding chemical additives [15] for fresh GRCs are among these solutions.

Recently, the use of nanomaterials such as carbon nanotubes (CNTs) has been suggested by many researchers to overcome the deficiency of cementitious composites [16, 17]. Having the very best mechanical, physical, electrical, and specific surface area makes CNT remarkable for researchers [18]. The carbon nanotube is an

allotrope of carbon and is classified in two groups as single-walled carbon nanotube (SWCNT) and multi-walled carbon nanotube (MWCNT) [19]. The physical and mechanical differences between SWCNT and MWCNT are compared in Table 1. CNT's usability in cementitious materials was first proposed by Brenner et al. [20] and patented in 2008. It is expected that calcium silicate hydrates (C-S-H) that hold a cementitious matrix together can be controlled by nano-scale CNTs [21]. However, more MWCNTs have been investigated in cementitious materials and studies on SWCNT-cementitious materials are rather limited.

Table 1. Differences between SWCNTs and MWCNTs [22]

	SWCNT	MWCNT
Diameter	0.5–3.0 nm	5–100 nm
Length	100 nm–1 cm	100 nm–1 cm
Typical Young's modulus	1.3 TPa	1.8 TPa
Tensile strength	Up to 53 GPa	Up to 63 GPa
Electrical conductivity	10000 S/cm	6000 S/cm
Heat conductivity	Max. 6000 W/m·K	Max. 3000 W/m·K

Limited number of representative studies on SWCNT-cement composites are summarized. Kang et al. [22] studied the mechanical properties of 0, 0.02, 0.04, and 0.06 wt.% SWCNT added cement composites. With the presence of TritonX-100 agent used as dispersion, it was concluded that both the compressive and flexural strength improved, while the increase in the SWCNT ratio without dispersing agent caused the strength to decrease. Li et al. [23] investigated the combined effects of SWCNT and graphene oxide on the cement. According to the flexural test results, 72.7 % increase has been observed in the strength of the cements containing SWCNT-GO. Separately, it was stated that the strength increased by

* Corresponding author. Tel.: +90-380-542-1133.

E-mail address: serkansubasi@duzce.edu.tr (S. Subasi)

51.2 % by GO and 26.3 % by SWCNTs. Jonathan et al. [24] studied the growth of cement hydration products on SWCNTs. It has been found that SWCNT accelerates the hydration reaction of C_3S in portland cement. First, it was stated that the morphology of both C_3A and C_3S hydration products is affected by the presence of SWCNT. In particular, nanotubes were rapidly coated with C-S-H, while the nanotubes were seen to act as nucleation sites for C_3S hydration products. The resulting structures remained on the surface of the cement grains, while those of the sonicated and delivered OPC samples grew from the grain surfaces to form typical C-S-H clusters.

It is important to improve the mechanical properties of GRCs whose demand is increasing day by day especially in shell element applications. In this study, it was aimed to examine the mechanical and microstructural properties of GRC-SWCNT composites produced by using different ratios of SWCNT to improve the micro and nanostructures of GRCs.

2. EXPERIMENTAL

2.1. Materials

CEM II / B-L 42,5 R White Portland limestone cement has been used as a binder material in premixed GRC mixtures. Silica sand (2–850 μm) suitable for GRC production has been used as filler material. As the aid binder material, calcined kaolin (CK) with 70.45 % SiO_2 , Al_2O_3 and Fe_2O_3 ratios has been used. According to the results of various studies, the positive effects of CK on cementitious mortars [25] have been confirmed. The specific gravity of the CK used is 2.52 g/cm^3 . The chemical components of the cement, CK, and silica sand (SS) used are given in Table 2.

Table 2. Chemical composition of mineral materials

Component	Cement, %	Silica sand, %	Calcined kaolin, %
SiO_2	17.46	98.57	59.78
Al_2O_3	3.27	0.00	10.23
Fe_2O_3	0.21	0.17	0.44
CaO	63.04	0.29	9.91
MgO	1.67	0.00	1.59
K_2O	0.34	0.16	0.90
Na_2O	0.30	0.00	0.05
SO_3	3.02	0.00	1.25
P_2O_5	0.04	0.01	0.04
TiO_2	0.09	0.12	0.15
Cr_2O_3	0.0021	0.0137	0.0186
Mn_2O_3	0.0042	0.0029	0.0077
LOI	11.00	0.39	16.24

Alkali resistant glass fiber (AR-GF) of 12 mm length and 14 μm diameter was used to increase tensile strength and prevent cracks. The specific gravity, tensile strength, and melting point of the AR-GF used were 2800 kg/m^3 , 2450 MPa and $800 \text{ }^\circ\text{C}$, respectively. In a previous study [26], it was confirmed that AR-GF can be used positively in sputtered GRC. In addition, if AR-GF is homogeneously dispersed, it can prevent the formation and development of

micro cracks in the shell elements. Vinyl acrylic copolymer (VA-CP) solution was used as an additive material to provide a homogeneous mixture and to obtain a denser composite [27]. Polycarboxylate ether-based plasticizer was used in all mixtures.

The paste shape SWCNT used in the study has beta-302 carrier and was provided by the TUBAL company. The concentrated carrier of this SWCNT consists of surfactant, stabilizing agent-alkylene glycol derivative and distyryle biphenyl derivative [28]. SEM image of SWCNT is given in Fig. 1. The carbon content of the SWCNT used was $99 \pm 1 \text{ wt.}\%$ and it had a diameter of 1–2 nm. The length of this material, which is very flexible and strong, is approximately 3000 times its diameter.

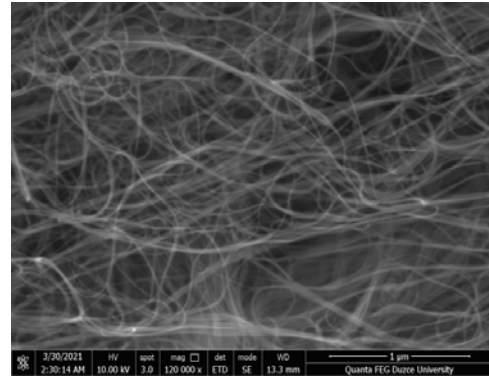


Fig. 1. SEM image of SWCNT

2.2. Mix design

GRCs are generally produced by spray and premix methods [29]. In this study, all mixtures were produced as a premix. Cement, aggregate, calcined kaolin, and glass fiber, which are the main materials of GRC, were dry mixed in the amounts in Table 3 for three minutes. The desired amount of SWCNT was added to 70 % of the mixing water. According to the information provided by the company, it is necessary to mix the material in a certain amount of water for a minimum of 20 minutes to disperse it. SWCNTs with dispersant added in black pieces were mixed in an impeller blade shape mixer at 2000 rpm. During the mixture, the dispersion success was tested by laying the sample taken with a glass baguette on paper. The best dispersion success was observed after 40 min. The dispersed carbon nanotube was added to the mixture and the mixing process continued for 3 minutes. In the next step dispersed carbon nanotubes were added while the mixture continued. Then, the superplasticizer (SP) was added with the remaining 30 % of the water and the mixing process was terminated after 2 minutes. The stages of the mixing procedure are schematically given in Fig. 2.

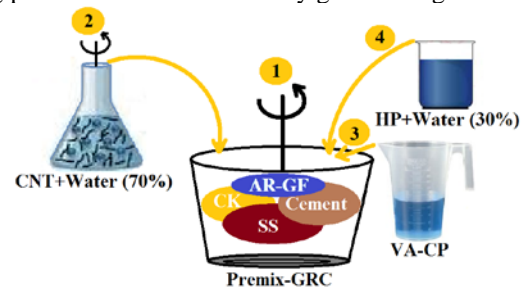


Fig. 2. A schematic view for the mixing procedure

Table 3. Mixture design and contents of mortars

No	Cement, g	Calcined kaolin, g	Silica sand, g	Vinyl acrylic, g	Glass fiber, vol.%	Superplasticizer, %wt	Water, g	SWCNT, wt.%
1	7340	306	7650	153	0	0.9	2440	0
2	7340	306	7638	153	2.5	0.9	2440	0.007
3	7340	306	7632	153	2.5	0.9	2440	0.010
4	7340	306	7626	153	2.5	0.9	2440	0.015
5	7340	306	7614	153	2.5	0.9	2440	0.020

The water/binder ratio was kept at 0.32 in all mixtures. HP was added as 0.9 % by the weight of cement. The prepared mixtures were poured into molds and removed from the molds after 24 hours, and the specimens were cured for 7 and 28 days.

2.3. Test methods

After the mixtures were prepared, a slump test was performed according to TS EN 1170-1 [30] to check their workability. This standard covers a test method that makes it possible to check the suitability of the water / cement ratio in glass fiber reinforced cement (GRC) and the workability of the mixture (suitability for pumpability and compression). The test is carried out by placing the mixture in a 55 mm high, 57 mm inner diameter pipe and lifting the pipe in a vertical direction. The average diameter of the circularly radiating mixture indicates the slump value.

7 and 28-day 50 mm cube specimens produced for the determination of compressive strength were tested according to the TS EN 196-1 [31] standard. Before the compressive strength test (28-day), the dry density and capillarity values of the same specimens have been specified according to TS EN 1170-6 [32]. Within the scope of this standard, the density of the GRC specimen is measured following the Archimedes principle. Also, to investigate the effect of SWCNT on the hardness of GRCs, the Leeb hardness test was performed on cube samples according to ASTM-A956 [33]. To determine the strength of composites to impact, tests following the [34] standard were carried out on 10 × 15 × 110 mm sized specimens.

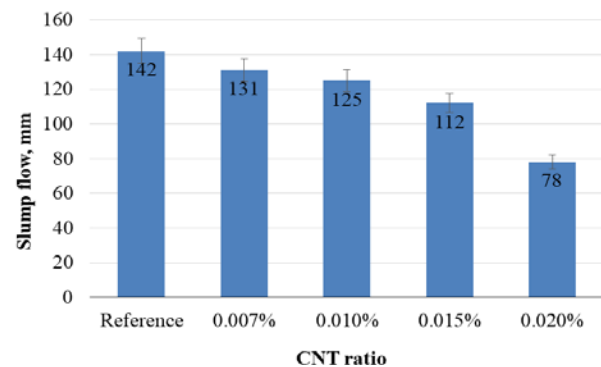
7 and 28-day 200 × 15 × 10 mm specimens were used to determine the flexural strength of composites and tested according to TS EN 1170-4 [35]. Direct tensile tests were carried out on 250 × 25 × 10 mm sized specimens according to TS EN 1394 [36]. For all experiments, three from each mixture were tested and average values were taken. Field Emission Scanning Electron Microscopy (FE-SEM) analyzes were performed to determine the morphological and internal structures of the produced GRC-CNT composites. FE-SEM is an advanced technology used to capture the microstructure image of the materials. FE-SEM is typically performed in a high vacuum because gas molecules tend to disturb the electron beam and the emitted secondary and backscattered electrons used for imaging. The SEM, EDX device used was the Quanta FEG 250 type of the FEI (Field Electron and Ion Company) producer, with high resolution Schottky Field Emission and magnification from 14 to 1 million. For FE-SEM analysis, samples were taken from the crack regions after compressive strength. Since cementitious materials are insulators, SEM images cannot be obtained at

the desired quality. Samples were first coated with a conductive material (Au/Pd) to obtain the desired images.

3. RESULTS AND DISCUSSION

3.1. Workability

The slump flow values of GRC-CNT composites are shown in Fig. 3. The SWCNT ratio had a significant effect on the slump flow. While the slump value of the reference was 142 mm, the slump value of the 0.02 wt.% SWCNT added mixture decreased by 45 % to 78 mm. Most studies [37, 38] have confirmed that the workability of MWCNT cement is reduced. The high specific surface area of CNTs is the main reason for reduced workability. Therefore, since SWCNTs have higher specific surface areas than MWCNTs, these nanomaterials can further affect the workability of cement. In one study [39], the interaction of CNTs with aluminate phases (mainly C₃A) and their ability to cause a reduction in the workability of the mixture was noted. In fresh concrete, the C₃A phase has a key role in affecting workability [38]. In the study of Makar and Chan [24], it has been reported that SWCNTs cause inhibition of C₃A formation. On the other hand, the rapid concentration of C-S-H on the SWCNT, which acts as the core, is another potential reason for workability to decline.

**Fig. 3.** Slump flow values of mixtures

3.2. Density and capillarity

The filler and nucleation effects of the CNTs can increase the density of the cement matrix and make it more compact [38]. Generally, the effects of MWCNT on the properties of cementitious materials have been studied, and research on the effect of SWCNT is very limited. Besides that, it has been noted in the literature that MWCNT has indefinite effects on the density of cementitious materials. It has been reported that increasing the density by adding MWCNT in [40, 41] studies, decreasing the density in [42] research, and being ineffective in [43]. In the study of Chaipanich et al. [41], the density of CNT added fly ash

mortar was 2.29, the density of only fly ash mortar was 2.19, and density of normal Portland cement mortar was 2.23 g/cm³. In this study, the density of 0.007 wt.%, 0.01 wt.% and 0.015 wt.% SWCNT added composites increased by 1 %, 1.3 % and 2 %, respectively (Fig. 4 a). However, the density of the composite containing 0.02 % SWCNT was reduced by 0.5 % compared to the reference. This is due to the low workability and the permanent voids that occur during insertion.

Rashad [37] reported that the three main advantages of using CNT in cementitious materials are reducing porosity, permeability and water absorption. In cementitious materials, the porosity ratio can be reduced and a denser matrix can be obtained by filling the voids between the hydration products with the condensed C-S-H on CNT. The 90 minute capillary test results of composites containing different amounts of SWCNT are compared in Fig. 4 b. Parallel relationship between capillarity and density values can be seen in Fig. 4. The weights of 0, 0.007, 0.01, 0.015 and 0.02 wt.% SWCNT added composites increased by 2.212, 0.972, 1.087, 0.865 and 2.320 %, respectively, after the test. The weight gain due to water absorption depends on the porosity ratio of the composites. Looking at the time-weight curves, the weight gain for all composites is more evident in the first 15 minutes. The capillary curve of the 0.015 % SWCNT added composite has continued at a lower speed compared to the others and has gradually fixed in the horizontal direction. The capillarity curve of the composite containing 0.02 % SWCNT has continuously increased due to the imperfections caused by the low consistency.

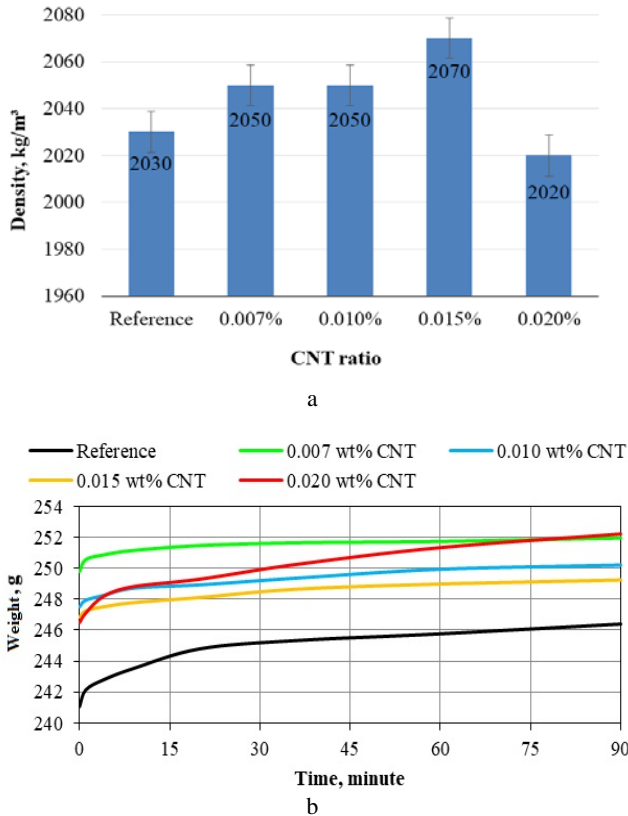


Fig. 4. Test results of composites: a – density; b – capillarity

3.3. Mechanical test results

Compressive, flexural and tensile strengths of 7 and 28-day old GRC-CNT composites are given in Fig. 5, Fig. 6 and Fig. 7, respectively. Considering all the mechanical test results, parallelism is observed between them. When the flexural and tensile test results are examined, it is understood that the age effect is more pronounced than the compressive strength. The average compressive, flexural and tensile strengths of the 28-day specimens have increased as 16 %, 38 % and 37 %, compared to 7-day, respectively. CNTs increase the hydration speed and accelerate the formation of C-S-H, so compressive strength is expected to improve at an early age [24]. The increase in the rate of SWCNT revealed that the age effect was more pronounced. Xu et al. [38], stated that some water molecules are absorbed by siphoning into the cavities of nano-tubes. As the CNT ratio increases, the amount of water absorbed increases. With the increase of the CNT ratio, the amount of water absorbed increases and the hydration rate slows down, so, logically the compressive strength increases further in older ages. With the increase of the CNT ratio up to 0.015 wt.%, the compressive strength increased, but when the CNT ratio became 0.02 wt.%, the compressive strength decreased to the strength level of the reference specimen. However, the compressive strengths of 28-day composites containing 0.007, 0.01, 0.015 and 0.02 % SWCNT increased compared to the reference as 0.04, 0.14, 0.62 and 0.19 %, respectively.

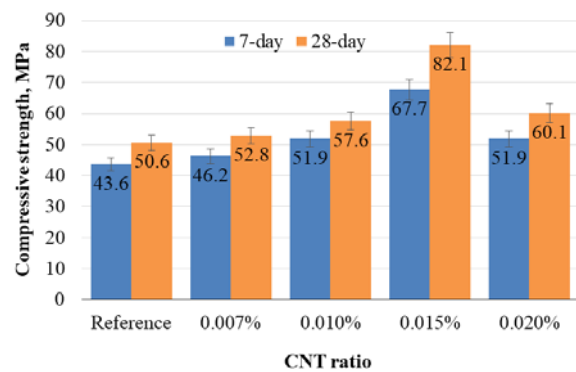


Fig. 5. 7 and 28-Day compressive strength results

Kang et al. [22] investigated the strength of 0, 0.02, 0.04 and 0.06 wt. % (by weight of cement) SWCNT added cement composites. The positive effect of SWCNT was observed in mixtures using dispersion additive. The maximum compressive strength has been obtained for the composite containing 0.06 wt.% SWCNT. Kerienè et al. [40] examined the effect of MWCNTs on non-autoclaved aerated concrete and autoclaved aerated concrete separately. According to the results of the mixture with different ratios of MWCNT, it has been reported that the maximum compressive strength belongs to the 0.02 wt.% nanotube added mixture, by an increase of 11.03 %. Also, reductions in shrinkage during the heating period have been detected. According to the research results of Musso et al. [44], there was deterioration in mechanical properties with functionalized CNTs, while a significant

improvement was achieved with both grown and annealed CNTs.

As with the compressive strength results, the flexural and tensile strength increased with the increase of the CNT ratio to 0.015 % and the strength decreased when the CNT ratio increased to 0.02 %. The flexural strength of composites containing 0.007, 0.01, 0.015 and 0.02 % SWCNT increased by 15, 26, 45 and 20 %, respectively. Kang and Al-Sabah produced 0.02–0.04 wt.% SWCNT (by weight of cement) added mortars and examined their mechanical strength. They reported 10–20 % positive effects of SWCNT on the flexural strength of mortars. Also, the tensile strength of the samples with the same mixtures increased by 17, 33, 56 and 32 %, respectively, compared to the reference. In this study, while the flexural strength of GRC-SWCNT composites was 9.78–14.18 MPa, it was reported as 4.50–9.95 MPa for the GRC matrix in different studies. [45, 46].

In many studies [47, 48], positive effects of CNTs on the flexural strength of cementitious materials have been reported. However, some inconsistencies regarding flexural strength have also been reported across studies. Inconsistencies in flexural strength may be related to the CNT dispersion and bonding property of CNT-cement. In CNT reinforced cementitious materials, the bond between CNT and cement is the most important factor for flexural strength. However, the CNT dispersion type, quality and property can significantly affect the bond mechanism. Considering these factors, it is useful to develop a probabilistic model for estimating flexural strength. Ramezani et al. [49], suggested a probabilistic model by using the Kelly-Tyson theory for the estimate of flexural strengths of CNT reinforced cement composites. The model suggests that the CNT aspect ratio ranges from 400 to 800, and the concentration of 0.08 wt.% to 0.18 wt.% (cement-wt) yields the highest flexural strength. Finally, model variables were validated by comparing them with experimental study variables. For example, with the increase in the CNT ratio in the composite, it was revealed that the age significance was more pronounced.

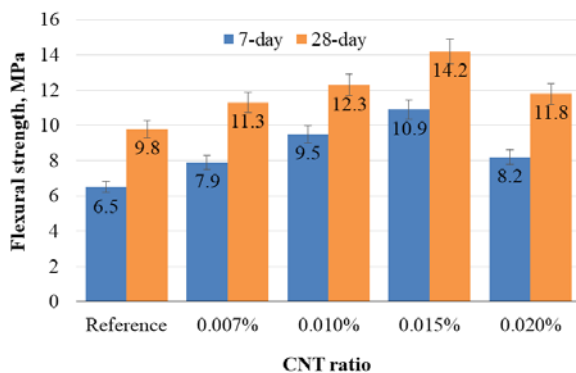


Fig. 6. 7 and 28-day flexural strength results

Since the general usage areas of GRCs are shell elements, tensile strength is also important. There are limited studies in the literature regarding the direct tensile strength of GRCs. Peled et al. [50], investigated the tensile strength of size stabilizing additive, acrylic polymer and blast furnace slag added GRCs, along with other mechanical properties. Among the tensile strengths of

2.8–7.6 MPa obtained for different mixtures, the biggest improvement has been observed for mixtures with acrylic polymer and slag addition. In a study conducted by Ali et al. [45], the split tensile strength of 0.5 vol.% fiber reinforced GRC composites at 28-180 days was obtained as 3.5–4.5 MPa. In this study, 7 and 28-day direct tensile strength for 2.5 vol.% glass fiber reinforced GRC matrix was obtained as 4.73 and 7.48 MPa, respectively. Maximum tensile strength has been reported as 11.64 MPa for 0.015 wt.% CNT added composite. The age effect was more pronounced in high CNT dosage composites on tensile strength as in compressive and flexural strength results. The age effect for 0.007 wt.% and 0.02 wt.% CNT added composites was 23 % and 62 %, respectively.

Relationships between the mechanical properties of composites were examined in Fig. 8. The correlation coefficient of over 80 confirms bilateral relationships. In the literature [51, 52], it is stated that the correlation coefficient should be at least 70 for the estimated model between the two factors to be suitable. Considering the equations in the figure, the flexural/compressive strength rate is higher than the others. This is compatible with some studies in the literature [45, 46]. Also, according to the correlation coefficients, $R = 0.9753$ proves that the equation between flexural-tensile is plausible than other equations. In Ali et al.'s study [45], the relationships of compressive- splitting tensile and compressive- flexural found for GRCs are given in Eq. 1 and Eq. 2, respectively. According to ACI Committee 363 [53], Eq. 3 and Eq. 4 are available for the relations of compressive- splitting tensile and compressive- flexural, respectively. In these equations, f_r is the flexural strength, f_c , compressive strength, and f_{sp} splitting tensile strength. These equations are generally more compatible for coarse aggregate concretes. According to the literature, the f_r/f_c ratio may be higher in fine aggregate concrete types. For example, in the study of Arslan et al. [54] and Aygormez et al. [55], f_c - f_r relations were obtained as Eq. 5 and Eq. 6, respectively, for geopolymer concretes.

$$f_{sp} = 0.604 \times \sqrt{f_c} ; \quad (1)$$

$$f_r = 0.755 \times \sqrt{f_c} ; \quad (2)$$

$$f_{sp} = 0.59 \times \sqrt{f_c} ; \quad (3)$$

$$f_r = 0.94 \times \sqrt{f_c} ; \quad (4)$$

$$f_r = 1.32 \times \sqrt{f_c} ; \quad (5)$$

$$f_r = 1.34 \times \sqrt{f_c} . \quad (6)$$

If the equations in Fig. 8 are written in $f_y = a \times \sqrt{f_x}$ format, the following equations can be suggested for premix GRCs. In these equations f_r , f_c and f_t are flexural, compressive and tensile strength, respectively.

$$f_r = 1.53 \times \sqrt{f_c} ; \quad (7)$$

$$f_t = 1.23 \times \sqrt{f_c} ; \quad (8)$$

$$f_t = 2.79 \times \sqrt{f_r} . \quad (9)$$

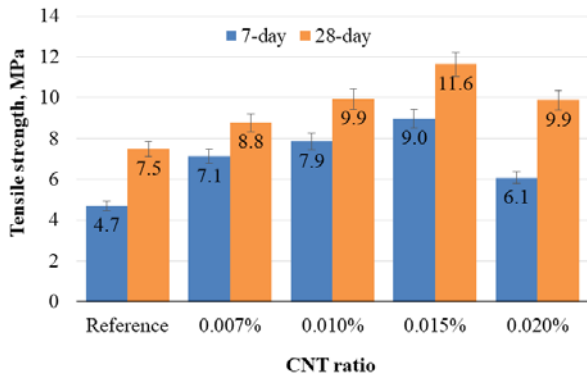


Fig. 7. 7 and 28-Day tensile strength results

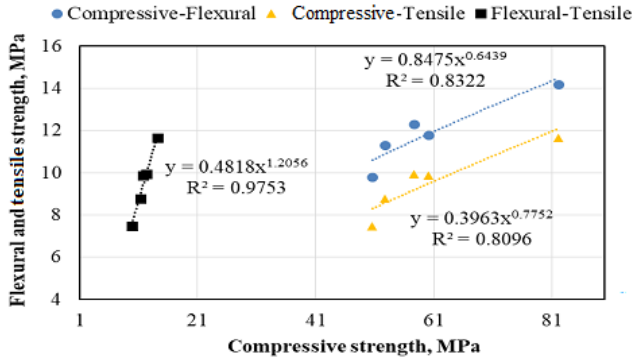


Fig. 8. Compressive-flexural, compressive-tensile and flexural-tensile strength relationships

3.3. Impact test results

To determine the impact strength of the produced GRC-SWCNT composites, the absorb energy values of the relevant specimens were read by using a device following the ISO 179-1 standard [34]. Impact strength values of the specimens have been calculated using Eq. 10 [56]. For statistical accuracy, 5 specimens from each mix were tested. The average absorbed energy and impact strength values obtained have been compared in Fig. 9.

$$a_{CU} = \frac{E_C}{h \times b} \quad (10)$$

where E_C is the absorbed energy (kJ); h , the thickness of the test specimen (m) and b is the width of the tests specimen (m).

The ISO 179-1 standard is generally a test method that determines the impact properties of polymeric materials [57, 58]. However, since the general usage areas of the GRC-SWCNT composites produced in this study are shell elements, it is useful to examine the impact behavior using this test method.

The impact strength and absorbed energy values of composites are given in Fig. 9. The impact properties of the 0.007, 0.001, 0.015 and 0.02 % SWCNT added composites has changed by 17.99, 40.84, 28.48 and 6.80 % compared to the reference. Its absorbed energy values vary between 3.12–4.72 J and impact strength values between 14.4–21.76 kJ/m². While 0.01 % SWCNT added composite showed the best impact properties, the impact properties of 0.02 % SWCNT added composite remained below the reference. On the contrary, according to all other

test results, maximum values were obtained for the 0.015 % SWCNT composite.

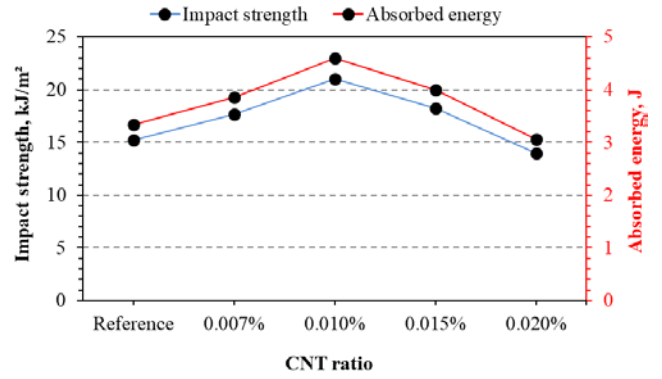


Fig. 9. Impact strength and absorbed energy of composites

3.4. Hardness test results

The Leeb hardness test, which is a non-destructive method, provides information about the hardness and estimated strength of construction materials such as stone and concrete [59, 60]. This method was used to obtain information about the hardness of SWCNT added GRC composites produced in this study. The results are compared in Fig. 10. The hardness value was obtained as 375 HL for the reference GRC specimen. No significant difference was observed between the hardness of the 0.007 wt.% SWCNT added composite and the reference. However, the hardness of 0.010 wt.% and 0.015 wt.% SWCNT added composites increased 7.2 % and 8.8 %, respectively, compared to the reference. This is because the SWCNTs form a three-dimensional network, preventing transverse deformations and micro cracks. In addition, the density of material in the Leeb hardness test method also significantly affects the values. Comparing the hardness values with the density and capillarity results in Fig. 4 confirms this. Pores smaller than 0.1 μ m are formed in mortars only in the presence of hydraulic phases (C-S-H) and remain empty due to their size. However, the presence of sorption pores in C-S-H is a common feature for both cement putties and mortars. Consequently, changes in porosity are affected by the presence of CSH and carbon nanotubes that increase the density of the gel phases [61]. The hardness of the 0.020 % SWCNT added composite has reduced by 2 % compared to the reference. The reason for this is the low density resulting from the reduced workability.

There are a few Leeb hardness studies on normal concretes, although limited. But there is no information about the Leeb hardness of GRCs. Song et al. [62] investigated the Leeb hardness of sodium silicate based concrete and normal C30 concrete and concluded that the average hardness value of normal concrete was 362.4 HL and that of sodium silicate based concrete was 405.6 HL. The hardness values of the 28-day GRC-SWCNT composites produced in this study were measured between 372.68 and 408.10 HL. Therefore, the results prove to be compatible when compared to normal concrete. Gomez-Heras et al. [63] stated that the finer the grain size, the higher the Leeb hardness. Also CK benefits to improve the surface hardness of concrete [64]. This situation is directly

related to the filling of finegrained minerals into micro and macropores [65].

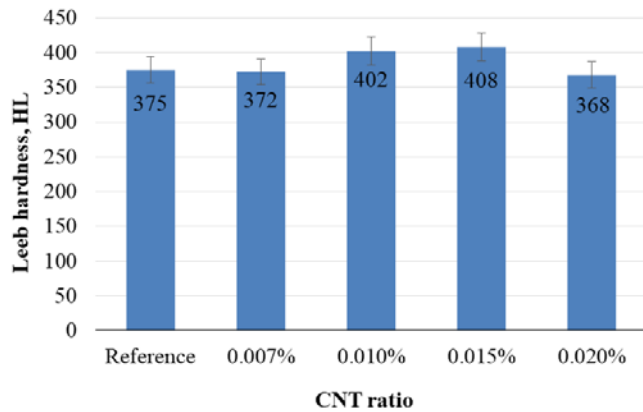
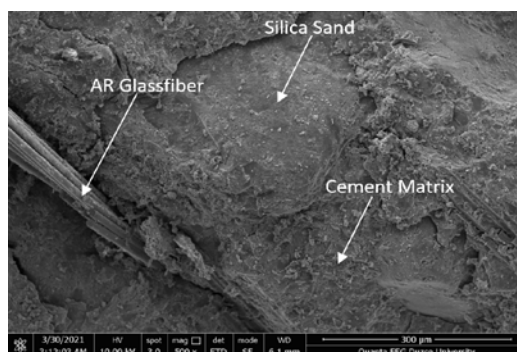


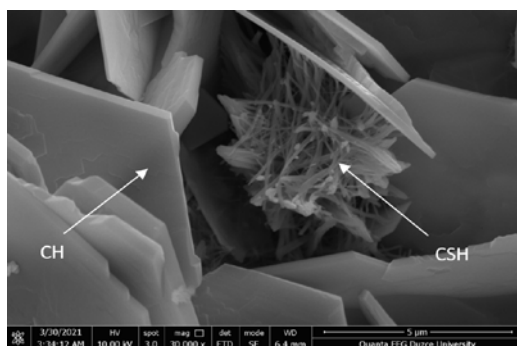
Fig. 10. Leeb hardness measured for GRC-SWCNT composites

3.4. SEM analysis

Field emission scanning electron microscopy (FE-SEM) images of pure GRC and SWCNT added composites are presented in Fig. 11 and Fig. 12, respectively. The image in Fig. 11 a was taken at 500 times magnification to display the glass fibers in the matrix. For the visibility of C-S-H and SWCNTs, 40000 and 120000 times magnified images were taken. While micro-cracks parallel to the fibers were observed in glass fiber composites, no micro-cracks were observed perpendicular to the fibers. If these cracks are not prevented, they can expand over time and compromise the integrity of the composite.



a



b

Fig. 11. FE-SEM images of pure GRC: a – at 500^x; b – at 30000^x

Considering the general condition of GRC concrete, a dense structure and good adherence between matrix and fiber are observed. In Fig. 11 b, at 30000 times

magnification, hexagonal crystals from cement products and needle-like products in between are observed. CSH phases between typical crystals exhibiting hexagonal morphology have been confirmed in [66] and [67]. Hydration of tricalcium silicate ($3\text{CaO}\cdot\text{SiO}_2$) in Portland cement-based materials is a process involving certain reactions. The most important of these reactions is the formation of portlandite ($\text{Ca}(\text{OH})_2$) and calcium-silicatehydrate (CSH) gel [68]. Portlandite is the result of hydrolysis of tricalcium (C_3S) and dicalcium (C_2S) silicates after a few hours when Portland cement is combined with water, forming hexagonal crystal plates of about $40\ \mu\text{m}$ in a solid phase. Portlandite constitutes 25 % of the solid phase of hydrated Portland cement [67]. CSH-gel is a cement product with many important engineering properties that ensure the strength of the matrix. There are two types of CH; hexagonal crystals and fine amorphous grains closely adsorbed on the CSH-gel surface [68].

Considering the FE-SEM images of the SWCNT added composites, it is observed that there is a good bond between SWCNT and C-S-H. In addition, the homogeneous distribution of nanotubes in the matrix is remarkable. The reason why SWCNTs look bright is because they are very good electrically conductive. In the FE-SEM image of the 0.015 % SWCNT added composite, it was observed that the crack below $1\ \mu\text{m}$ at 40000 magnification was firmly bonded with SWCNTs. SWCNTs, which act as bridges for cement products, prevent the development of micro cracks in the matrix and protect the composite from possible damage. This is important in terms of mechanical and durability for cementitious materials. Fibrous products with diameters of about $50\ \text{nm}$ observed in the images (see Fig. 12 a and b) are known to be CSH, according to the morphology of the hydration products of the cement [69]. The interaction of SWCNTs with these products may be the reason for the decrease in the workability of the mixtures. The FE-SEM image of the composite containing the highest dosage of SWCNT (Fig. 12 d) shows a good network formation on the matrix surface of the nanotubes. However, the agglomeration of nanotubes may explain the decrease in the mechanical strength of this composite.

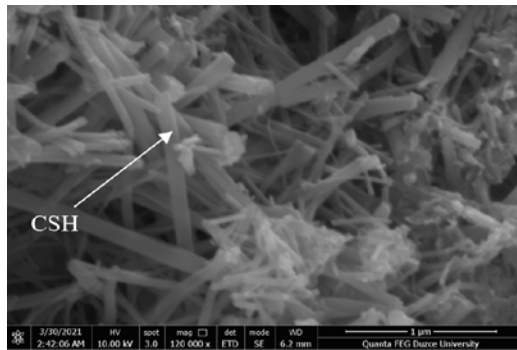
4. CONCLUSIONS

Five different GRC-SWCNT composites including reference were produced, their mechanical and physical properties were examined and their microstructures were characterized. The following conclusions have been reached by comparing the obtained values with the literature in detail;

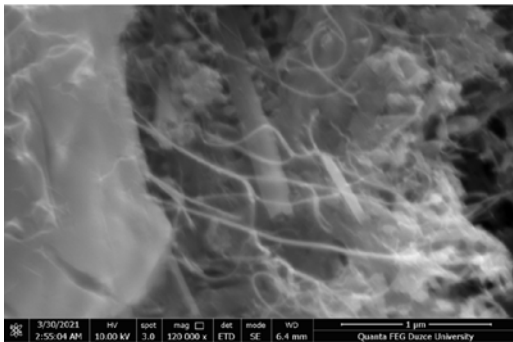
The addition of SWCNTs to GRC significantly affected workability. This was explained by the fact that SWCNTs have a very high specific surface area. Also, the interaction between SWCNTs and hydration products of cement was confirmed by FE-SEM images as the other reason for this situation.

In this study, the 28-day maximum compressive, flexural and tensile strengths were obtained for 0.015 wt.% SWCNT added composites. It has been confirmed in the FE-SEM images that SWCNTs act as a bridge for micro-cracks, causing an increase in strength. In addition to the

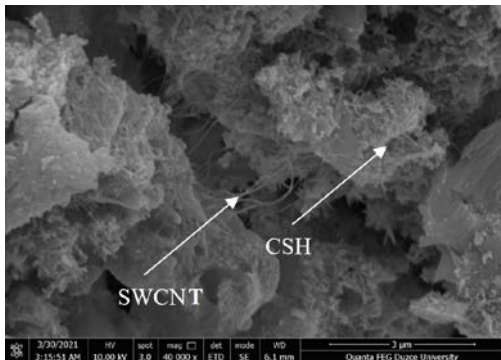
harmony of all the obtained results, there were linear relationships, especially between the mechanical results. While the SWCNT ratio increased to 0.015 wt.%, the density increased a little and decreased as it increased to 0.02 wt.%.



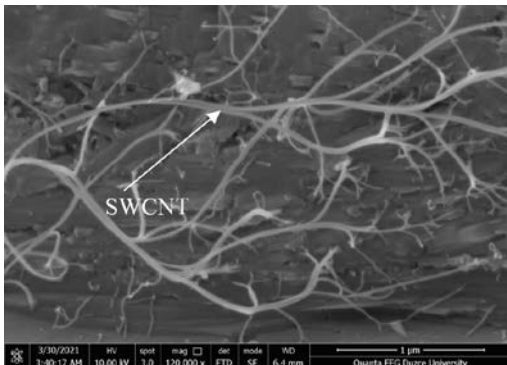
a



b



c



d

Fig. 12. FE-SEM images of GRC composites containing: a–0.007; b–0.010; c–0.015; d–0.020 wt.% of SWCNT

Capillarity curves obtained depending on the time also showed parallelism with the density values.

Considering the impact strength and absorption energy results of composites, 0.01 wt.% SWCNT added composites showed the most satisfactory performance.

Except for of 0.02 wt.%, the Leeb hardness values of the composites were improved by the addition of SWCNT. SWCNTs form a network, preventing micro cracks, filling pores, and the increase in density in composites as a result of the development of CSH products explains this situation.

Acknowledgments

This study was carried out within the scope of the project coded ARGE2017-9 of Fibrobeton R&D Center. Thank you to Fibrobeton Company for their support.

REFERENCES

1. **Yang, S., Yu, M., Dong, K., Yang, Y.** Properties of Alkali-resistant Glass Fiber Reinforced Coral Aggregate Concrete *Materials* 13 (16) 2020: pp. 1–16. <https://doi.org/10.3390/MA13163450>
2. **Topbas, A., Tulen, F., Marasli, M., Kohen, B.** A Prefabricated GFRC-UHPC Shell Pedestrian Bridge *IASS Annual Symposium Structural Membranes* 2019.
3. **Lipatov, Y.V., Gutnikov, S.I., Manylov, M.S., Lazoryak, B.I.** Effect of ZrO₂ on The Alkali Resistance and Mechanical Properties of Basalt Fibers *Inorganic Materials* 48 2012: pp. 751–756. <https://doi.org/10.1134/S0020168512060106>
4. **Enfedaque, A., Paradela, L.S., Sánchez-Gálvez, V.** An Alternative Methodology to Predict Aging Effects on the Mechanical Properties of Glass Fiber Reinforced Cements (GRC) *Construction and Building Materials* 27 2012: pp. 425–431. <https://doi.org/10.1016/j.conbuildmat.2011.07.025>
5. **Sivakumar, A., Santhanam, M.** Mechanical Properties of High Strength Concrete Reinforced with Metallic and Non-Metallic Fibres *Cement and Concrete Composites* 29 2007: pp. 603–608. <https://doi.org/10.1016/j.cemconcomp.2007.03.006>
6. **Scheffler, C., Zhandarov, S., Mäder, E.** Alkali Resistant Glass Fiber Reinforced Concrete: Pull-Out Investigation of Interphase Behavior Under Quasi-Static and High Rate Loading *Cement and Concrete Composites* 84 2017: pp. 19–27. <https://doi.org/10.1016/j.cemconcomp.2017.08.009>
7. **Zhu, Z., Zhang, C., Meng, S., Shi, Z., Tao, S., Zhu, D.** A Statistical Damage Constitutive Model Based on the Weibull Distribution for Alkali-Resistant Glass Fiber Reinforced Concrete *Materials* 12 2019: pp. 1–17. <https://doi.org/10.3390/ma12121908>
8. **Mirza, F.A., Soroushian, P.** Effects of Alkali-Resistant Glass Fiber Reinforcement on Crack and Temperature Resistance of Lightweight Concrete *Cement and Concrete Composites* 24 2002: pp. 223–227. [https://doi.org/10.1016/S0958-9465\(01\)00038-5](https://doi.org/10.1016/S0958-9465(01)00038-5)
9. **Xiaochun, Q., Xiaoming, L., Xiaopei, C.** The Applicability of Alkaline-Resistant Glass Fiber in Cement Mortar of Road Pavement: Corrosion Mechanism And Performance Analysis *International Journal of Pavement Research and Technology* 10 2017: pp. 536–544. <https://doi.org/10.1016/j.ijprt.2017.06.003>

10. **Marasli, M.** Developing the Estimation Model of Flexural and Compressive Strengths Using the Maturity Index Method in Glass Fiber Reinforced Concrete. *Düzce University, Graduate School of Natural and Applied Sciences. Master thesis*, 2019.
11. **Majumdar, A.J., Nurse, R.W.** Glass Fibre Reinforced Cement *Materials Science and Engineering* 15 1974: pp. 107–127.
[https://doi.org/10.1016/0025-5416\(74\)90043-3](https://doi.org/10.1016/0025-5416(74)90043-3)
12. **Ferreira, J.G., Branco, F.A.** Structural Application of Grc in Telecommunication Towers *Construction and Building Materials* 21 2007: pp. 19–28.
<https://doi.org/10.1016/j.conbuildmat.2005.08.003>
13. **Purnell, P., Short, N.R., Page, C.L.** A Static Fatigue Model for the Durability of Glass Fibre Reinforced Cement *Journal of Materials Science* 36 2001: pp. 5385–5390.
<https://doi.org/10.1023/A:1012496625210>
14. **Liang, W., Cheng, J., Hu, Y., Luo, H.** Improved Properties of GRC Composites Using Commercial E-Glass Fibers With New Coatings *Materials Research Bulletin* 37 2002: pp. 641–646.
[https://doi.org/10.1016/S0025-5408\(02\)00700-6](https://doi.org/10.1016/S0025-5408(02)00700-6)
15. **Marikunte, S., Aldea, C., Shah, S.** Durability of Glass Fiber Reinforced Cement Composites: Effect of Silica Fume and Metakaolin *Advanced Cement Based Materials* 5 1997: pp. 100–108.
16. **Kordkheili, H.Y., Shehni, S.E., Niyatzade, G.** Effect of Carbon Nanotube on Physical and Mechanical Properties of Natural Fiber/Glass Fiber/Cement Composites *Journal of Forestry Research* 26 2015: pp. 247–251.
<https://doi.org/10.1007/s11676-014-0003-y>
17. **Kordkheili, H.Y., Hiziroglu, S., Farsi, M.** Some of the Physical and Mechanical Properties of Cement Composites Manufactured From Carbon Nanotubes and Bagasse Fiber *Materials and Design* 33 2012: pp. 395–398.
<https://doi.org/10.1016/j.matdes.2011.04.027>
18. **Chong, K.P., Garboczi, E.J.** Smart and Designer Structural Material Systems *Progress in Structural Engineering and Materials* 4 2002: pp. 417–430.
<https://doi.org/10.1002/pse.134>
19. **Delzeit, L.D.** U.S. Patent No. 6,858,197 Patent and Trademark Office, 2009.
20. **Brenner, M., Mariputtana, A., Michael, K., Li, G.Y.** U.S. Patent No. 2008/0134942 A1 Patent and Trademark Office, 2008.
21. **Morsy, M.S., Alsayed, S.H., Aqel, M.** Hybrid Effect of Carbon Nanotube and Nano-Clay on Physico-Mechanical Properties of Cement Mortar *Construction and Building Materials* 25 2011: pp. 145–149.
<https://doi.org/10.1016/j.conbuildmat.2010.06.046>
22. **Kang, J., Al-sabah, S.** Effect of Single-Walled Carbon Nanotubes on Strength Properties of Cement Composites *Materials* 13 (36) 2020: pp. 1–21.
<https://www.mdpi.com/1996-1944/13/6/1305>
23. **Li, X., Wei, W., Qin, H., Hu, Y.** Co-Effects of Graphene Oxide Sheets and Single Wall Carbon Nanotubes on Mechanical Properties of Cement *Journal of Physics and Chemistry of Solids* 85 2015: pp. 39–43.
<https://doi.org/10.1016/j.jpics.2015.04.018>
24. **Makar, J.M., Chan, G.W.** Growth of Cement Hydration Products on Single-Walled Carbon Nanotubes *Journal of the American Ceramic Society* 92 2009: pp. 1303–1310.
<https://doi.org/10.1111/j.1551-2916.2009.03055.x>
25. **Said-Mansour, M., Kadri, E.H., Kenai, S., Ghrici, M., Bennaceur, R.** Influence of Calcined Kaolin on Mortar Properties *Construction and Building Materials* 25 2011: pp. 2275–2282.
<https://doi.org/10.1016/j.conbuildmat.2010.11.017>
26. **Ates, A.O., Khoshkholghi, S., Tore, E., Marasli, M., İlki, A.** Sprayed Glass Fiber-Reinforced Mortar with or without Basalt Textile Reinforcement for Jacketing of Low-Strength Concrete Prisms *Journal of Composites for Construction* 23 2019: pp. 04019003.
[https://doi.org/10.1061/\(asce\)cc.1943-5614.0000922](https://doi.org/10.1061/(asce)cc.1943-5614.0000922)
27. **Kharazian, H.A., Zare, M.R., Noktehdan, M., Sedaghatdoost, A.** Effect of Water-Based Acrylic Copolymer on Void Systems of Cementitious Repair Mortar *Case Studies in Construction Materials* 11 2019: pp. e00261.
<https://doi.org/10.1016/j.cscm.2019.e00261>
28. **TUBALL.** Technical Data Sheet of TUBALL™ MATRIX 302. V02_201905:0–2, 2018.
29. **Töre, E., Ateş, A.O., Khoshkholghi, S., Maraslı, M., İlki, A.** Reinforcement for Increasing Ductility with Spray GRC and Basalt Textile Reinforced GRC *8th National Earthquake Engineering Conference, Istanbul, Turkey* 2015: pp. 905–913.
30. **TS EN 1170-1.** Measuring the Matrix Consistence “Slump Test” Method *Turkish Standard*, 1999: ICS 91.100:1–2.
31. **TS EN 196-1.** Methods of Testing Cement—Part 1: Determination of Strength *Turkish Standard*, 2005.
32. **TS EN 1170-6.** Dry Density Testing by Water Absorption and Immersion *Turkish Standard ICS 91.100:1–6*, 1999.
33. **ASTM A956.** Standard Test Method for Leeb Hardness Testing of Steel Products *American Society for Testing and Materials*, 2006.
34. **ISO 179-1.** Plastics—Determination of Charpy Impact Properties. Part 1: Non-instrumented Impact Test. *ISO, Geneva International Standards Organization*, 2010.
35. **TS EN 1170-4.** Precast Concrete Products-Test Method for Glass-Fibre Reinforced Cement-Part 4: Determination of Flexural Strength. *Turkish Standard*, 1999.
36. **TS EN 1394.** Direct Tensile Strength Test Method. *Turkish Standard*, 1999.
37. **Rashad, A.M.** Effect of Carbon Nanotubes (Cnts) on The Properties of Traditional Cementitious Materials *Construction and Building Materials* 153 2017: pp. 81–101.
<https://doi.org/10.1016/j.conbuildmat.2017.07.089>
38. **Xu, S., Lyu, Y., Xu, S., Li, Q.** Enhancing the Initial Cracking Fracture Toughness of Steel-Polyvinyl Alcohol Hybrid Fibers Ultra High Toughness Cementitious Composites by Incorporating Multi-Walled Carbon Nanotubes *Construction and Building Materials* 195 2019: pp. 269–282.
<https://doi.org/10.1016/j.conbuildmat.2018.10.133>
39. **Raki, L., Beaudoin, J., Alizadeh, R., Makar, J., Sato, T.** Cement and Concrete Nanoscience and Nanotechnology *Materials* 3 2010: pp. 918–942.
<https://doi.org/10.3390/ma3020918>
40. **Kerienė, J., Kligys, M., Laukaitis, A., Yakovlev, G., Špokauskas, A., Aleknevičius, M.** The Influence of Multi-Walled Carbon Nanotubes Additive on Properties of Non-Autoclaved and Autoclaved Aerated Concretes *Construction and Building Materials* 49 2013: pp. 527–535.
<https://doi.org/10.1016/j.conbuildmat.2013.08.044>
41. **Chaipanich, A., Nochaiya, T., Wongkeo, W.,**

- Torkittikul, P.** Compressive Strength and Microstructure of Carbon Nanotubes-Fly Ash Cement Composites *Materials Science and Engineering A* 527 2010: pp. 1063–1067. <https://doi.org/10.1016/j.msea.2009.09.039>
42. **Hu, Y., Luo, D., Li, P., Li, Q., Sun, G.** Fracture Toughness Enhancement of Cement Paste With Multi-Walled Carbon Nanotubes *Construction and Building Materials* 70 2014: pp. 332–338. <https://doi.org/10.1016/j.conbuildmat.2014.07.077>
43. **Del Carmen Camacho, M., Galao, O., Baeza, F. J., Zornoza, E., Garcés, P.** Mechanical Properties and Durability of Cnt Cement Composites *Materials* 7 2014: pp. 1640–1651. <https://doi.org/10.3390/ma7031640>
44. **Musso, S., Tulliani, J.M., Ferro, G., Tagliaferro, A.** Influence of Carbon Nanotubes Structure on the Mechanical Behavior of Cement Composites *Composites Science and Technology* 69 2009: pp. 1985–1990. <https://doi.org/10.1016/j.compscitech.2009.05.002>
45. **Ali, B., Raza, S.S., Hussain, I., Iqbal, M.** Influence of Different Fibers on Mechanical and Durability Performance of Concrete With Silica Fume *Structural Concrete* 2020: pp. 1–16. <https://doi.org/10.1002/suco.201900422>
46. **Ali, B., Qureshi, L.A.** Influence of Glass Fibers on Mechanical and Durability Performance of Concrete With Recycled Aggregates *Construction and Building Materials* 228 2019: pp. 116783. <https://doi.org/10.1016/j.conbuildmat.2019.116783>
47. **Gdoutos, E.E., Konsta-Gdoutos, M.S., Danoglidis, P.A.** Portland Cement Mortar Nanocomposites at Low Carbon Nanotube and Carbon Nanofiber Content: a Fracture Mechanics Experimental Study *Cement and Concrete Composites* 70 2016: pp. 110–118. <https://doi.org/10.1016/j.cemconcomp.2016.03.010>
48. **Danoglidis, P.A., Konsta-Gdoutos, M.S., Gdoutos, E.E., Shah, S.P.** Strength, Energy Absorption Capability and Self-Sensing Properties of Multifunctional Carbon Nanotube Reinforced Mortars *Construction and Building Materials* 120 2016: pp. 265–274. <https://doi.org/10.1016/j.conbuildmat.2016.05.049>
49. **Ramezani, M., Kim, Y.H., Sun, Z.** Probabilistic Model for Flexural Strength of Carbon Nanotube Reinforced Cement-Based Materials *Composite Structures* 253 2020: pp. 112748. <https://doi.org/10.1016/j.compstruct.2020.112748>
50. **Peled, A., Jones, J., Shah, S.P.** Effect of Matrix Modification on Durability of Glass Fiber Reinforced Cement Composites *Materials and Structures/Materiaux et Constructions* 38 2005: pp. 163–171. <https://doi.org/10.1617/14091>
51. **Dehghanpour, H., Yilmaz, K.** Investigation of Specimen Size, Geometry and Temperature Effects on Resistivity of Electrically Conductive Concretes *Construction and Building Materials* 250 (2) 2020: pp. 118864. <https://doi.org/10.1016/j.conbuildmat.2020.118864>
52. **Dehghanpour, H., Yilmaz, K.** The Relationship Between Resistances Measured by Two-Probe, Wenner Probe and C1760-12 Astm Methods in Electrically Conductive Concretes *SN Applied Sciences* 2 (1) 2020: pp. 1–10. <https://doi.org/10.1007/s42452-019-1811-7>
53. **ACI Committee 363R.** State-of-the-Art Report on High-Strength Concrete. *ACI, Detroit*, 2010.
54. **Arslan, A.A., Uysal, M., Yilmaz, A., Al-mashhadani, M.M., Canpolat, O., Şahin, F., Aygörmez, Y.** Influence of Wetting-Drying Curing System on the Performance of Fiber Reinforced Metakaolin-Based Geopolymer Composites *Construction and Building Materials* 225 2019: pp. 909–926. <https://doi.org/10.1016/j.conbuildmat.2019.07.235>
55. **Aygörmez, Y., Canpolat, O., Al-mashhadani, M.M., Uysal, M.** Elevated Temperature, Freezing-Thawing and Wetting-Drying Effects on Polypropylene Fiber Reinforced Metakaolin Based Geopolymer Composites *Construction and Building Materials* 235 2020: pp. 117502. <https://doi.org/10.1016/j.conbuildmat.2019.117502>
56. **Shagwira, H., Mwema, F., Mbuya, T., Adediran, A.** Dataset on Impact Strength, Flammability Test and Water Absorption Test for Innovative Polymer-Quarry Dust Composite *Data in Brief* 29 2020: pp. 105384. <https://doi.org/10.1016/j.dib.2020.105384>
57. **Takahashi, Y., Chai, J., Tan, S.C.** Effect of Water Storage on the Impact Strength of Three Glass Fiber-Reinforced Composites *Dental Materials* 22 2006: pp. 291–297. <https://doi.org/10.1016/j.dental.2005.04.035>
58. **Yang, X.G., Duan, D.L., Zhang, X., Jiang, S.L., Li, S., Zhang, H.C.** Impact Behavior of Polyetheretherketone/Nickel Foam Co-Continuous Composites *Journal of Materials Engineering and Performance* 28 2019: pp. 6380–6390. <https://doi.org/10.1007/s11665-019-04360-0>
59. **Mishra, D.A., Basu, A.** Estimation of Uniaxial Compressive Strength of Rock Materials by Index Tests Using Regression Analysis and Fuzzy Inference System *Engineering Geology* 160 2013: pp. 54–68. <https://doi.org/10.1016/j.enggeo.2013.04.004>
60. **Ortega, J.A., Gómez-Heras, M., Perez-López, R., Wohl, E.** Multiscale Structural and Lithologic Controls in the Development of Stream Potholes on Granite Bedrock Rivers *Geomorphology* 204 2014: pp. 588–598. <https://doi.org/10.1016/j.geomorph.2013.09.005>
61. **Konstantopoulos, G., Koumoulos, E., Karatza, A., Charitidis, C.** Pore and Phase Identification Through Nanoindentation Mapping and Micro-Computed Tomography in Nanoenhanced Cement *Cement and Concrete Composites* 114 2020: pp. 103741. <https://doi.org/10.1016/j.cemconcomp.2020.103741>
62. **Song, Z., Xue, X., Li, Y., Yang, J., He, Z., Shen, S., Zhang, N.** Experimental Exploration of the Waterproofing Mechanism of Inorganic Sodium Silicate-Based Concrete Sealers *Construction and Building Materials* 104 2016: pp. 276–283. <https://doi.org/10.1016/j.conbuildmat.2015.12.069>
63. **Gomez-Heras, M., Benavente, D., Pla, C., Martinez-Martinez, J., Fort, R., Brotons, V.** Ultrasonic Pulse Velocity as a Way of Improving Uniaxial Compressive Strength Estimations from Leeb Hardness Measurements *Construction and Building Materials* 261 2020: pp. 119996. <https://doi.org/10.1016/j.conbuildmat.2020.119996>
64. **Pangdaeng, S., Sata, V., Aguiar, J.L., Pacheco-Torgal, F., Chindapasirt, J., Chindapasirt, P.** Bioactivity Enhancement of Calcined Kaolin Geopolymer with CaCl₂ Treatment *Science Asia* 42 2016: pp. 407–414. <https://doi.org/10.2306/scienceasia1513-1874.2016.42.407>
65. **García-del-Cura, M.Á., Benavente, D., Martínez-Martínez, J., Cueto, N.** Sedimentary Structures and Physical Properties of Travertine and Carbonate Tufa Building Stone *Construction and Building Materials* 28 2012: pp. 456–67.

<https://doi.org/10.1016/j.conbuildmat.2011.08.042>

66. **Hartmann, A., Khakhutov, M., Buhl, J.C.** Hydrothermal Synthesis of Csh-Phases (Tobermorite) Under Influence of Ca-Formate *Materials Research Bulletin* 51 2014: pp. 389–396.
<https://doi.org/10.1016/j.materresbull.2013.12.030>
67. **Polychroniadis, E.K., Oral, A.Y., Ozer, M.** SEM Investigation of Microstructures in Hydration Products of Portland Cement *2nd International Multidisciplinary Microscopy and Microanalysis Congress: Proceedings of InterM, October* 164 2015: pp. 16–19.
68. **Yaseen, S.A., Yiseen, G.A., Poon, C.S., Li, Z.** Influence of Seawater on the Morphological Evolution and the Microchemistry of Hydration Products of Tricalcium Silicates (C3S) *ACS Sustainable Chemistry and Engineering* 8 2020: pp. 15875–15887.
<https://doi.org/10.1021/acssuschemeng.0c04440>
69. **Nguyen, T.N.M., Yoo, D.Y., Kim, J.J.** Cementitious Material Reinforced by Carbon Nanotube-Nylon 66 Hybrid Nanofibers: Mechanical Strength and Microstructure Analysis *Materials Today Communications* 23 2020: pp. 100845.
<https://doi.org/10.1016/j.mtcomm.2019.100845>



© Subasi et al. 2022 Open Access This article is distributed under the terms of the Creative Commons Attribution 4.0 International License (<http://creativecommons.org/licenses/by/4.0/>), which permits unrestricted use, distribution, and reproduction in any medium, provided you give appropriate credit to the original author(s) and the source, provide a link to the Creative Commons license, and indicate if changes were made.